Technical Note

JOURNAL OF ENDOVASCULAR THERAPY
An official publication of the International Society of Endovascular Specialists
A SAGE Publication

# EVAR Guided by 3D Image Fusion and $CO_2$ DSA: A New Imaging Combination for Patients With Renal Insufficiency

Journal of Endovascular Therapy
2015, Vol. 22(6) 912–917

DOI: 10.1177/1526602815605468
www.jevt.org
SAGE

**Giasemi Koutouzi, MD[1], Olof Henrikson, MD[1], Håkan Roos, MD[2], Karin Zachrisson, MD[1], and Mårten Falkenberg, MD, PhD[1]**

**Abstract**

**Purpose:** To present a new combination of imaging techniques that helps reduce the use of iodinated contrast during endovascular aneurysm repair (EVAR) procedures in patients with renal insufficiency. **Technique:** Relevant anatomical structures are marked in the preprocedure computed tomography (CT) angiogram. A 3D-3D image fusion between the preprocedure CT and an intraprocedure cone-beam CT is performed in order to overlay anatomical information on live fluoroscopy. Verification of the correct overlay matching (or adjustment if necessary) is based on carbon dioxide ($CO_2$) digital subtraction angiograms (DSA) instead of iodine DSA. The stent-graft is placed and deployed based on the overlaid information. Correct device placement is finally verified with conventional contrast angiography. **Conclusion:** The combination of 3D image fusion of a preoperative CT with live fluoroscopy and $CO_2$ DSA verification is feasible and sufficient for guidance of abdominal EVAR. This method minimizes the use of iodinated contrast media, protecting residual function in the setting of preexisting renal insufficiency.

**Keywords**

3D image fusion, carbon dioxide angiography, digital subtraction angiography, endovascular aneurysm repair, image guidance, renal failure

## Introduction

Endovascular aneurysm repair (EVAR) has become the treatment of choice for abdominal aortic aneurysms (AAA), particularly in elderly patients with comorbidity. Renal insufficiency is common in patients with atherosclerotic aneurysms and is an independent risk factor for mortality after aneurysm repair. During EVAR, the kidneys may be further damaged by the large doses of nephrotoxic iodinated contrast medium[1,2] injected close to the renal arteries before, during, and after stent-graft deployment. Minimization of iodinated contrast is therefore important when performing EVAR on patients with renal insufficiency.

Three-dimensional (3D) image fusion of a preoperative computed tomography (CT) scan with an intraoperative cone-beam computed tomography (CBCT) image can facilitate endovascular navigation by overlaying important CT-derived anatomical landmarks on the fluoroscopy screen, thereby limiting the need for repeated contrast injections during procedures.[3,4] However, the overlay accuracy is not always perfect due to introduction of stiff guidewires that straighten curved vessels, involuntary patient movements, and other factors.[5,6] There is thus still a need to confirm the accuracy of the overlaid information by using 2D digital subtraction angiograms (DSAs) with iodinated contrast.

Gaseous carbon dioxide ($CO_2$) can be safely used as a negative intra-arterial contrast agent below the diaphragm,[7,8] but the image quality of $CO_2$ DSAs is usually inferior to conventional DSA with iodinated contrast due to gas buoyancy, bolus fragmentation, and poorer vessel demarcation. When used in combination, 3D image fusion and $CO_2$ DSA complement each other and may eliminate the need for iodinated contrast, even in complex EVAR procedures.

[1]Department of Radiology, Sahlgrenska University Hospital, Gothenburg, Sweden
[2]Department of Vascular Surgery, Sahlgrenska University Hospital, Gothenburg, Sweden

**Corresponding Author:**
Giasemi Koutouzi, Department of Radiology, Sahlgrenska University Hospital, Bruna Stråket 11B Plan 2, Gothenburg, 41345, Sweden.
Email: giasemi.koutouzi@vgregion.se

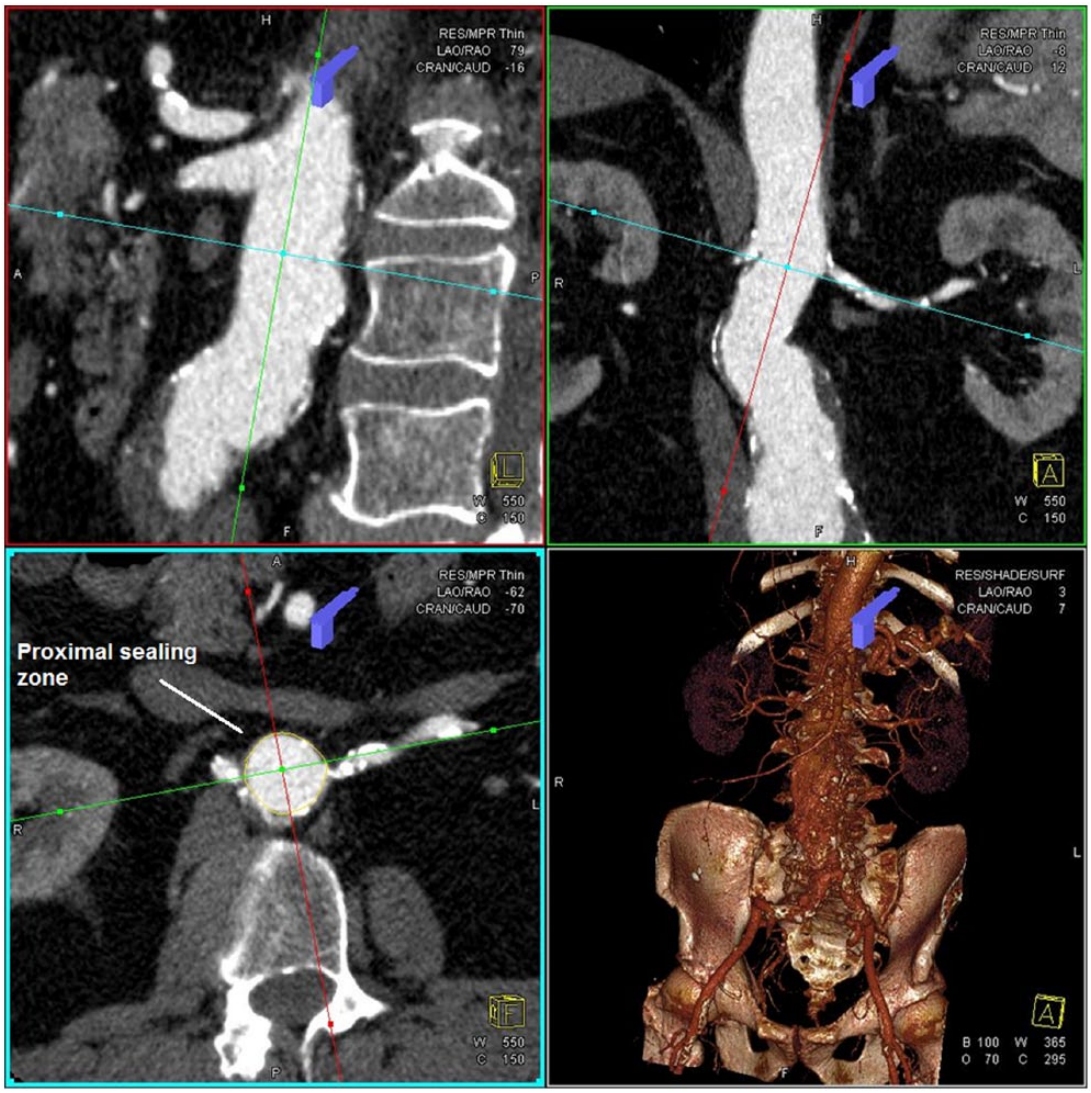


**Figure 1.** Screen layout of the workstation software used for case planning and 3D image fusion. The views of this preoperative computed tomography scan are clockwise from bottom left: axial, sagittal, coronal, and a volume rendering reconstruction. Landmarks such as planned proximal sealing zone are marked on the multiplanar reconstructions.

## Technique

Relevant anatomical structures are marked in the preprocedure CT angiogram (CTA). A 3D-3D fusion of the preprocedure CT with a noncontrast intraprocedure CBCT is done so that the marked structures can be overlaid on the live fluoroscopy image for guidance. The accuracy of the overlay is checked based on $CO_2$ DSA acquisitions and adjustments are made if required. The stent-graft is placed and deployed based on the overlaid information. The correct device placement is finally verified with conventional iodine angiography.

### *CT Marking and CBCT*

Our hybrid room is equipped with a multiaxis robotic C-arm system together with a tiltable angiography table and a dedicated postprocessing workstation (Artis Zeego and Syngo XWP; Siemens Healthcare, Forchheim, Germany). Thin slices of the preoperative CT are loaded in the postprocessing workstation, and anatomical structures of interest are marked on multiplanar reconstructions (Figure 1) using a dedicated 3D visualization and processing application (Syngo InSpace; Siemens Healthcare). Rings are drawn around the origins of the visceral vessels and a larger ring is

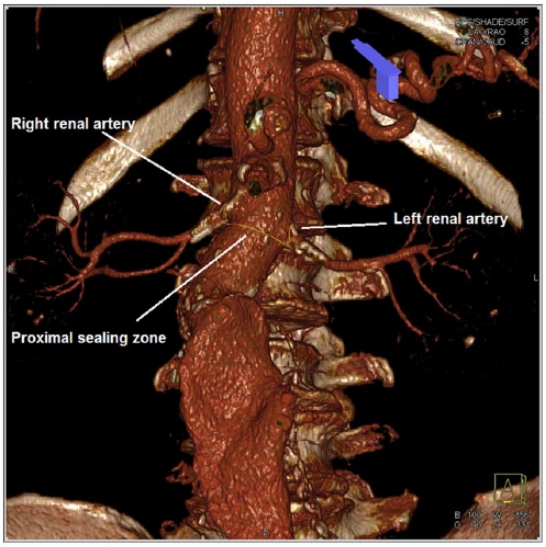


**Figure 2.** Volume-rendered reconstruction of the preoperative computed tomography scan of a patient with infrarenal aortic aneurysm. Endovascular aneurysm repair case planning identifies the origins of the renal arteries and the predicted proximal sealing zone for the aortic stent-graft just below the renal arteries.

drawn in the aorta perpendicular to its centerline at the optimal cranial extension of the aortic stent-graft (Figure 2). Where relevant, the aortic and iliac bifurcations are also marked.

CBCT without contrast is performed after the patient has been positioned on the operating table. During image acquisition, the C-arm equipped with a 30×400-cm flat-panel detector in either landscape or portrait orientation rotates around the patient on a 200° trajectory. The CBCT protocol used at our institution (5s DCT Body Care) acquires 248 projection images (0.8°/image) at a configured detector dose of 0.36 μGy. The projection images are automatically transferred to the workstation, where they are reconstructed to CT-like images with an isotropic voxel size of 0.5 mm. The cylindrical volume captured by a CBCT has a diameter of 25 cm and a height of 19 cm with the detector in landscape mode (19 cm and 25 cm, respectively, in portrait mode). To provide the best conditions for the following 3D fusion process, the patient should be centered on the table so that the spine is in the ISO center of the system, the iliac spines are visible in the caudal end of a frontal view, and the lumbar vertebrae are visible in the lower aspect of a lateral view.

## *Fusion of CT and CBCT*

Fusion of the datasets is performed with dedicated 3D-3D registration software (Syngo InSpace 3D3D Fusion; Siemens Healthcare) in a semiautomatic, 2-step approach using an intensity value–based normalized mutual information algorithm. First, an automatic registration is activated, followed by a manual adjustment process. As the content of the 2 volumes usually differs significantly (a contrast-filled CT is registered with a noncontrast CBCT), the result of the automatic registration is often insufficient. For a successful registration, which results in an accurate overlay of the vessel landmarks on live fluoroscopy, a good registration of the bony landmarks should serve as a starting point, while the manual fine adjustment should focus on the aortic calcifications, the aortic outline, aneurysms, and the ostia of visceral vessels. Depending on the accuracy of the initial automatic registration, the process of 3D image fusion can last from a few seconds to 5 minutes.

## *Overlay on Fluoroscopy*

Information from the fused dataset is then overlaid on the live fluoroscopic image using Syngo iPilot Dynamic for intraoperative guidance. There are several visualization options. The entire CT dataset can be superimposed or certain enhanced segments or only the markings of critical structures. At our institution, we prefer to overlay only the markings (rings) from the CT in order not to obscure intravascular devices. The overlay adapts dynamically to changes of position of the table, C-arm angulations, and the image zoom. Patient motion or changes of the anatomy are not taken into account.

## *$CO_2$ DSA*

We use the same technique for $CO_2$ angiography that has been described by others.[7,8] In brief, an angiographic catheter is positioned at the region of interest. $CO_2$ is injected either by hand with a syringe or by using a dedicated $CO_2$ injector. The syringe or the injector is flushed twice with $CO_2$ prior to filling the final volume to evacuate all air. For hand injection, a closed 1-way stopcock separates the $CO_2$-filled syringe from the catheter. Pressure is raised in the syringe with one hand, acquisition is started, and when the first subtracted image appears on the screen, $CO_2$ is released by opening the stopcock with the other hand. With this technique, all the $CO_2$ in the syringe is injected within 1 to 2 seconds. We use the following volumes of $CO_2$: 50 mL in the aorta, 30 mL in the common iliac, and 10–15 mL when the catheter is in the renal or hypogastric arteries. Acquisition programs for $CO_2$ DSA have a high frame rate (>6 frames/s), as the gas propagates quickly in the vessels, and a high kilovoltage to lower the skin dose but keep the contrast discrimination.

After each $CO_2$ DSA, any discrepancy in position between visualized vascular structures and the overlaid

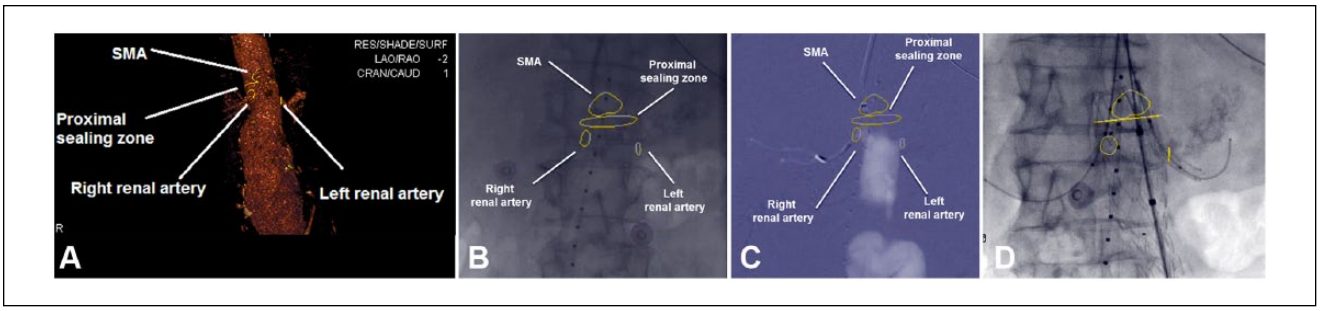


**Figure 3.** (A) Multiplanar reconstructions and volume rendering images from preoperative computed tomography angiography (CTA) of a 75-year-old man with juxtarenal abdominal aortic aneurysm; 3-dimensional graphics identify the renal arteries, the superior mesenteric artery (SMA), and the proximal landing zone just below the SMA ostium. (B) Graphics from the CTA are overlaid and continuously projected on the fluoroscopy screen for intraoperative guidance. (C) The overlaid CTA-derived ring-guided catheterization of the right renal artery. Carbon dioxide angiography with opacification of the aorta and the right renal artery confirms the correct position of the catheter. (D) Parallel stent-grafts to both renal arteries and the main bifurcated stent-graft are placed immediately below the SMA.

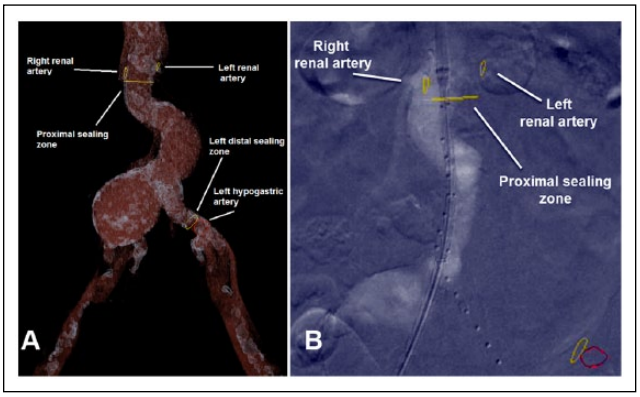


**Figure 4.** (A) Segmented volume-rendered reconstruction from the preoperative computed tomography (CT) of an 81-year-old man with right common iliac aneurysm. Note that even the preoperative CT is unenhanced. Case planning with 3-dimensional graphics marking the location of the proximal landing zone, renal arteries, left distal landing zone, and left hypogastric artery. (B) Carbon dioxide angiography with opacification of the aorta. CT-derived graphics are overlaid on the fluoroscopy image. There is a slight misalignment sideways between the $CO_2$ angiography and the overlaid markings. This was adjusted before stent-graft deployment.

markings is checked and, if necessary, adjusted manually. This is done by sliding and/or rotating the overlay over the fluoroscopic image until there is a perfect match between the markings and the corresponding points of interest (visceral ostia).

## *Illustrative Cases*

The first patient is a 75-year-old man on dialysis who still had some residual renal function to spare. The glomerular filtration rate (GFR) was 15 mL/min/1.73 $m^2$. He had a 65-mm juxtarenal aneurysm (Figure 3A) and was treated with parallel stent-grafts to both renal arteries (double chimneys), with the main bifurcated stent-graft placed immediately below the superior mesenteric artery (SMA; Figure 3B–D). The renal arteries were engaged from bilateral arm accesses guided by the overlaid rings. Correct positioning of each catheter was confirmed with $CO_2$ injection (Figure 3C), and the overlay position was adjusted to the actual anatomy if required. An aortic ring perpendicular to the centerline and just below the origin of the SMA aided placement of the main stent-graft. Craniocaudal C-arm angulation was adjusted so that the ring converged to a straight line, ensuring optimal projection of the aortic segment (Figure 3D). Completion angiography with 9 mL of iodinated contrast (240 mg I/mL) confirmed correct positioning of the stent-graft, patency of the visceral vessels, and no endoleak.

The second patient was an 81-year-old man with a GFR of 22 mL/min/1.73 $m^2$ and a 60-mm right common iliac aneurysm. The origins of the renal and hypogastric arteries were marked on the CT, as was optimal stent-graft coverage, with rings perpendicular to the vessel centerline (Figure 4A). Initially, the right hypogastric artery was embolized from a contralateral access, using the marking of its orifice for localization. A $CO_2$ DSA before deployment of the bifurcated aortic stent-graft showed that the overlay needed a slight sideways adjustment (Figure 4B) before the stent-graft was deployed. Completion angiography with 20 mL of iodinated contrast (240 mg I/mL) confirmed a successful procedure.

The third patient was a 76-year-old man with a GFR of 34 mL/min/1.73 $m^2$, and a 58-mm infrarenal aortic aneurysm. The renal arteries and the proximal landing zone for the aortic stent-graft were marked, and correct positions were confirmed with $CO_2$ DSA before deploying the stent-graft

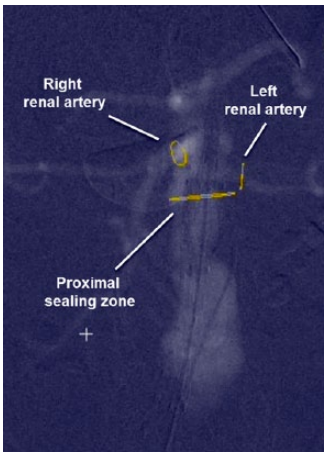


**Figure 5.** Carbon dioxide angiography in a 66-year-old man with infrarenal abdominal aortic aneurysm. Computed tomography–derived graphics mark the position of the proximal landing zone and the renal arteries.

(Figure 5) successfully, as confirmed by completion angiography with 20 mL of iodinated contrast (200 mg I/mL).

In all cases, catheterization and stent-graft deployment was guided by image fusion and $CO_2$ DSA, using a mean 3.7 grams of iodinated contrast per patient for completion angiography.

## Discussion

Renal insufficiency stands out as one of the most ominous predictors of mortality after aortic repair.[9,10] In open repair, the kidneys can be further damaged by the extensive surgical trauma, including aortic cross-clamping with resulting flux of reperfusion metabolites, and in some cases direct renal ischemia when suprarenal clamping is necessary. Endovascular repair is less traumatic by nature, and aortic occlusion times are usually very short, usually less than a minute. However, endovascular repair can also be harmful to the kidneys, mainly due to the nephrotoxic iodinated contrast medium used for orientation.

Using 3D image fusion, anatomical structures derived from preoperative imaging can be projected on the fluoroscopy screen to aid both standard and complex EVAR procedures.[11] Fusion techniques are developing quickly, and they are likely to become more accurate and user-friendly in the near future. The main challenges include visualization of critical anatomical features, reduction of radiation doses, and compensation for structural changes that occur during the intervention. For EVAR, we prefer visualization of vessel structures with simple markings, such as rings around vessels, as these are easily distinguished and cause minimal visual interference with the live fluoroscopic image. Radiation doses are relatively high for CBCT (mean effective dose 4.3 mSv, range 1.1–7.4 mSv),[12] but on the other hand, fusion overlays have been shown to reduce the number of contrast exposures needed for EVAR procedures.[13,14] Some systems allow two 2D exposures at different angles for volume fusion with 3D images, further reducing the total dose of radiation. In future, compensation for structural changes may be solved by automated organ recognition and image tracking,[15] but until then, operators will require a means of verifying the accuracy of overlaid structures and of making appropriate adjustments during procedures. The standard way to do this for vascular procedures is with intermittent exposures enhanced by iodinated contrast. In this report, we suggest that iodinated contrast should be replaced with $CO_2$ when treating patients with renal insufficiency.

Angiography with $CO_2$ was pioneered in the 1980s by Hawkins,[8] and since then it has been an alternative to iodinated contrast for some applications. $CO_2$ should not be used as an arterial contrast agent in sites above the diaphragm because of the risk of gas embolism of the spinal, coronary, and cerebral arteries. The most useful features of $CO_2$ are its lack of toxicity and its buoyancy, sometimes delineating upward-running vessels even better than water-soluble iodinated contrast. In 2012, Criado et al[7] published their experience of $CO_2$ angiography as the preferred angiographic contrast agent for EVAR in 114 consecutive patients. They concluded that $CO_2$-guided EVAR is technically feasible and safe, eliminating or reducing the need for iodinated contrast.

In our experience, the 2 techniques, 3D image fusion and $CO_2$ DSA, complement each other, and the combination is particularly useful in patients with marginal renal function. The combined technique allows both standard and complex EVAR procedures to be performed without any nephrotoxic contrast at all. In our 3 cases, iodinated contrast was used only for completion angiograms, but this could be replaced with additional $CO_2$-enhanced acquisitions, as suggested by Criado et al,[7] or with perioperative ultrasound.

## Conclusion

The combination of 3D image fusion with $CO_2$ DSA can be used to minimize the need for nephrotoxic iodinated contrast medium during EVAR in patients with renal insufficiency.

### Declaration of Conflicting Interests

The author(s) declare no potential conflicts of interest with respect to the research, authorship, and/or publication of this article.

### Funding

The author(s) received no financial support for the research, authorship, and/or publication of this article.

## References


1. Walsh SR, Tang TY, Boyle JR, et al. Renal consequences of endovascular abdominal aortic aneurysm repair. *J Endovasc Ther*. 2008;15:73–82.
2. Tepel M, Aspelin P, Lameire N. Contrast-induced nephropathy: a clinical and evidence-based approach. *Circulation*. 2006;113:1799–1806.
3. Maurel B, Hertault A, Sobocinski J, et al. Techniques to reduce radiation and contrast volume during EVAR. *J Cardiovasc Surg (Torino)*. 2014;55(2 suppl 1):123–131.
4. Tacher V, Lin M, Desgranges P, et al. Image guidance for endovascular repair of complex aortic aneurysms: comparison of two-dimensional and three-dimensional angiography and image fusion. *J Vasc Interv Radiol*. 2013;24: 1698–1706.
5. Maurel B, Hertault A, Gonzalez TM, et al. Evaluation of visceral artery displacement by endograft delivery system insertion. *J Endovasc Ther*. 2014;21:339–347.
6. Kauffmann C, Douane F, Therasse E, et al. Source of errors and accuracy of a two-dimensional/three-dimensional fusion road map for endovascular aneurysm repair of abdominal aortic aneurysm. *J Vasc Interv Radiol*. 2015;26:544–551.
7. Criado E, Upchurch GR, Young K, et al. Endovascular aortic aneurysm repair with carbon dioxide–guided angiography in patients with renal insufficiency. *J Vasc Surg*. 2012;55: 1570–1575.
8. Hawkins IF. Carbon dioxide digital subtraction angiography. *AJR Am J Roentgenol*. 1982;139:19–24.
9. Ohrlander T, Dencker M, Dias NV, et al. Cardiovascular predictors for long-term mortality after EVAR for AAA. *Vasc Med*. 2011;16:422–427.
10. Van Eps RG, Leurs LJ, Hobo R, et al. Impact of renal dysfunction on operative mortality following endovascular abdominal aortic aneurysm surgery. *Br J Surg*. 2007;94:174–178.
11. Dijkstra ML, Eagleton MJ, Greenbeg RK, et al. Intraoperative C-arm cone-beam computed tomography in fenestrated/branched aortic endografting. *J Vasc Surg*. 2011;53:583–590.
12. Sailer AM, Schurik GW, Wildberger JE, et al. Radiation exposure of abdominal cone beam computed tomography. *Cardiovasc Intervent Radiol*. 2015;38:112–120.
13. McNally MM, Scali ST, Feezor RJ, et al. Three-dimensional fusion computed tomography decreases radiation exposure, procedure time, and contrast use during fenestrated endovascular aortic repair. *J Vasc Surg*. 2015;61:309–316.
14. Hertault A, Maurel B, Midulla M, et al. Minimizing radiation exposure during endovascular procedures: basic knowledge, literature review, and reporting standards. *Eur J Vasc Endovasc Surg*. 2015;50:21–36.
15. Fernandes AT, Apisarnthanarax S, Yin L, et al. Comparative assessment of liver tumor motion using cine-magnetic resonance imaging versus 4-dimensional computed tomography. *Int J Radiat Oncol Biol Phys*. 2015;91:1034–1040.